

An fMRI-Compatible Multi-Configurable Handheld Response System Using an Intensity-Modulated Fiber-Optic Sensor*

Behnaz Jarrahi^{1,2,3}, Student Member, IEEE, Johann Wanek², Ulrich Mehnert², and Spyros Kollias³

Abstract—Functional magnetic resonance imaging (fMRI) data should be interpreted in combination and in the context of relevant behavioral measurements. However, the strong magnetic environment of MRI scanner and the supine position of participants in the scanner significantly limit how participants' behavioral responses are recorded. This paper presents the design of a low-cost handheld response system (HRS) with a multi-configurable optomechanical design that utilizes a reflective-type intensity modulated fiber-optic sensor (FOS) and a programmable visual interface to accurately gather participants' behavioral responses during an fMRI experiment. Considering the effects of an input unit design on the participants' performance efficiency across age groups and physical and neurological (dis)ability, the optomechanical system is designed to provide flexibility in the range of an input module with easy change-out feature. Specifically, the input unit can be configured as a binary module such as push buttons or as an analog input device including a scrolling wheel, and one-dimensional joystick (lever arm). To achieve MRI-compatibility, all parts of the unit that are used inside the scanner bore are built from nonferromagnetic and off-the-shelf plastic materials. The MRI compatibility was evaluated on a 3.0 Tesla MRI scanner running echo planar imaging (EPI) and the average time-variant signal-to-noise ratio (tSNR) loss is limited to 2%.

I. INTRODUCTION

Functional magnetic resonance imaging (fMRI) represents an effective method to study brain function, since it can noninvasively measure neural activity using blood oxygenation level dependent (BOLD) or arterial spin labeling (ASL) perfusion contrast. Behavioral data acquired jointly with brain images can be applied retrospectively during post-processing to improve the detection of brain activity in the fMRI time series, and are often used to model the expected hemodynamic response function [1].

Due to their small size, invulnerability to electromagnetic interference (EMI), and lack of electromagnetic susceptibility (EMS), optical fiber-based sensing techniques have been used in various fMRI applications, including motor response and force measurements [2], [3]. At present, there are some commercial providers that offer fiber-optic-based devices

*This research was supported by the Swiss National Science Foundation under grant No. 135774

¹B. Jarrahi is with the Department of Information Technology and Electrical Engineering, Swiss Federal Institute of Technology (ETH) Zurich, CH-8049 Zurich, Switzerland, and also with the Institute of Neuroradiology, University Hospital Zurich, CH-8091 Zurich, Switzerland, and the Spinal Cord Injury Center, Balgrist University Hospital, CH-8008 Zurich, Switzerland; Phone: +41 44 255 56 03; (email: jarrahib@ethz.ch).

²J. Wanek, and U. Mehnert are with the Spinal Cord Injury Center, Balgrist University Hospital, CH-8008 Zurich, Switzerland; (email: jwanek@paralab.balgrist.ch, umehnert@paralab.balgrist.ch).

³S. Kollias is with the Institute of Neuroradiology, University Hospital Zurich, CH-8091 Zurich, Switzerland; (email: kollias@dmr.usz.ch).

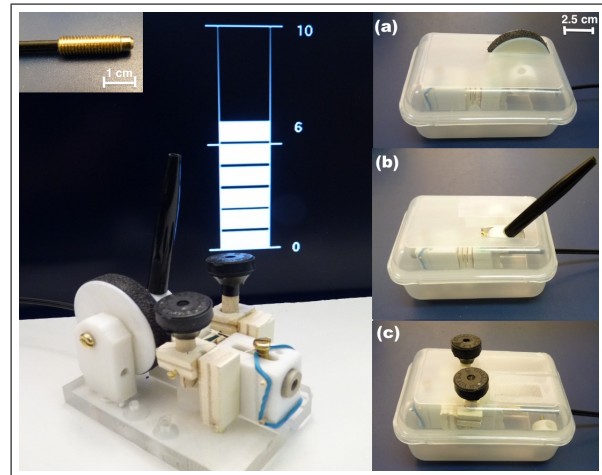


Fig. 1. HRS prototype with a programmable visual interface. Configurable input modules include (a) scrolling wheel, (b) lever arm (1-DOF joystick), and (c) push buttons. Inset shows close-up of the fiber optic sensor probe.

for behavioral measurements during fMRI. However, they typically are expensive (US\$2000 - 10000 in 2012), limited to one configuration, and usually require specialized stimulus control software. Consequently, this paper focuses on the design of a low-cost, multi-configurable handheld response system (HRS) with a programmable visual interface for use in fMRI experiments (Fig. 1).

II. DESIGN REQUIREMENTS AND SPECIFICATIONS

The design requirements for a behavioral measurement device for fMRI can be split up into critical design parameters (Table 1) and non-critical elements (Table 2). The most critical design parameter is the fMRI compatibility of the device which is explained in detail in [4], and embraces safety, conservation of MR image quality, and preservation of device functionality, reliability and precision of performance.

TABLE 1
CRITICAL DESIGN PARAMETERS FOR HRS

Parameter	Type	Specification
fMRI-compatibility	MR Image Artifacts	$\leq 5\%$ every time
	Magnetically Induced Force	$\theta_{Deflection} \leq 45^\circ$ ^a
	Magnetically Induced Torque	$< (\text{largest dimension} \times \text{device gravity force})$ ^b
Safety	Heating and Induced Voltage	heating effect $\leq 1^\circ\text{C}$ ^c
	Specific Absorption Rate (SAR)	$\leq 4 \text{ W/kg}$
Performance	Precision of Measurements	$\pm 5\%$ every time
	Reliability of Optical Signal	$\pm 5\%$ every time

a. ASTM F2052 b. A STM F2213 c. ASTM F2182

TABLE 2
NON-CRITICAL DESIGN PARAMETERS FOR HRS

Parameter	Type	Specification
Ergonomics	Size	Length = 10 to 15 cm ^a
		Thickness = 3 to 4 cm ^b
	Force	Power grip ≤ 21.35 N ^b
		Pinch grip ≤ 9.78 N ^b
Torque	Rotating tool ≤ 1.35 N.m ^c	
Mechanical factors	Maintenance	≤ 6 months
	Service Life	> 5 years
	Weight	≤ 1 kg

a. [5] b. [6] c. [7]

Other design parameters include the mechanical and ergonomic factors such as the comfort level during prolonged use in supine position, and the convenience of performance for different types of participants (e.g., children, adults, disabled users). The MRI environment is quite restrictive and participants can only provide feedback in limited ways. Older subjects, and patients with a physical or neurological impairment can find such tasks challenging especially because most behavioral measurement devices depend on the participants' strength, speed and range of movement when responding. For example, in a point-and-click task Trewin & Pain found that 70% of participants with motor disabilities had error rates greater than 10% and many pressed the button unintentionally before reaching the target [8]. Similar result was found by Smith et al. who examined the influence of age-related changes in the processing speed, visuo-spatial abilities and motor coordination required to use a mouse [9]. Other studies have shown the effect of the control-display gain¹ on the user performance [10]. In general, maximum acceptable force for repetitive exertion is 30% of a maximum voluntary contraction (MVC) [11]. From this perspective, the design of an input device not only depends on task requirements and environment compliancy, but also on participants (dis)ability level. Only few times the construction of MR-compatible devices has been approached with regards to ergonomics. Since *No Design Fits All*, we considered an adaptive design approach by incorporating multiple configurations to extend the range of participants one might consider for an fMRI experiment.

III. SYSTEM ARCHITECTURE

The system we have developed is a hand-held device (12.5 × 9 × 6 cm) that functions as peripheral hardware for any IBM-compatible PC. It consists of four elements: 1) a multi-configurable optomechanical unit; 2) a driver circuit board designed to operate the electronics of the sensor; 3) a data acquisition card interfaced with a Windows XP platform PC; and 4) a custom-made operating software for stimulus generation, as well as subject response collection and timing.

¹Control-display gain is defined as the relationship between the force applied on a control device (i.e., an input device) and movement of its control element (i.e., cursor on the display screen).

A. Optomechanical unit

The optomechanical unit of HRS consists of a reflective-type intensity modulated fiber-optic sensor (FOS) with a built-in light emitting diode (LED), optical amplifier, analog/digital conversion unit, and analogue voltage-output photodiode (FWDK 10U84Y0, Baumer Electric, Switzerland); an adjustable 10 m plastic-sheathed flexible fiber-optic cable with two optical fibers as transceivers (FUE 500C1003, Baumer Electric, Switzerland); a movable 5-mm diameter circular brass highly-reflective plate that is placed inside a hollow cylindrical tube perpendicular to the fiber tip. Each fiber has a tip diameter of 2.2 mm and is inserted in a 24 mm long brass pipe with an external diameter of 4.5 mm to form a sensor probe (top left inset of Fig. 1). The technical specifications of the HRS intensity-modulated FOS are summarized in Table 3.

TABLE 3
SPECIFICATIONS OF THE HRS INTENSITY-MODULATED FOS

Parameter type	Specification
Sensing distance	25 mm
Light source	Pulsed red LED
Wave length	680 nm
Voltage supply range	10.8 to 26.4 VDC
Max. supply current	20 mA
Offset	0.75 to 1.5 V
Analog voltage output	1.0 to 5.0 VDC
Response time	Adjustable from 1 to 50 ms

The input device integrates the sensor probe in a plastic case with the maneuvering elements (e.g., buttons, joystick, and wheel) and has a purely mechanical retraction mechanism using a rubber band. To prevent image artifacts and other issues related to the non-MRI-compatibility of the build-in components of the sensor, only the input device including the sensor probe is inside the MRI room, while the sensor body is placed in the adjacent control room.

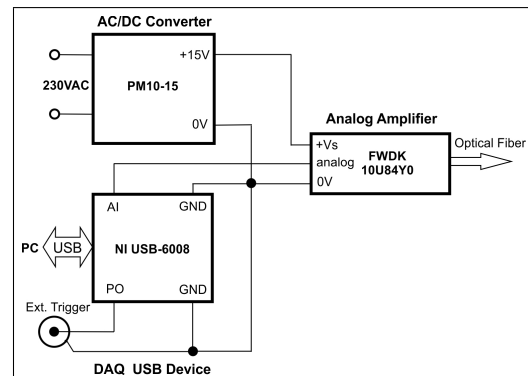


Fig. 2. HRS circuit board including power supply, DAQ, and amplifier

B. Driver circuit board

The circuit board includes a power supply for the FOS, an interface card and the FWDK 10U84Y0 amplifier as shown in Fig. 2. A 15V AC-to-DC converter (PM10-15, Mean Well Inc., CA, USA) provides required power to the HRS sensor.

C. Interface card

A 12-bit multifunction USB data acquisition card (DAQ USB-6008, National Instruments, TX, USA) is used as an interface to sample signals from FOS. During fMRI, it detects the TTL signals outputted by the scanner to trigger the start of a user-defined task (i.e., response recording).

D. The operational software

MATLAB (The MathWorks, MA, USA) with the Data Acquisition Toolbox™ is used to acquire and record the data. Once the system is initialized, the Data Acquisition Toolbox command *getdata* takes the acquired signal and saves it in a MATLAB variable. A custom MATLAB script quickly processes the raw signal, and uses a previously acquired calibration data to convert the data value from voltage to a relative displacement of a reflective surface, which then saves it in a .mat file. Once the data has been processed, another MATLAB script draws visual stimuli consisting of a visual analogue scale and a moving bar using Psychophysics Toolbox, an OpenGL-based MATLAB toolbox. A block diagram of the system software is presented in Fig. 3.

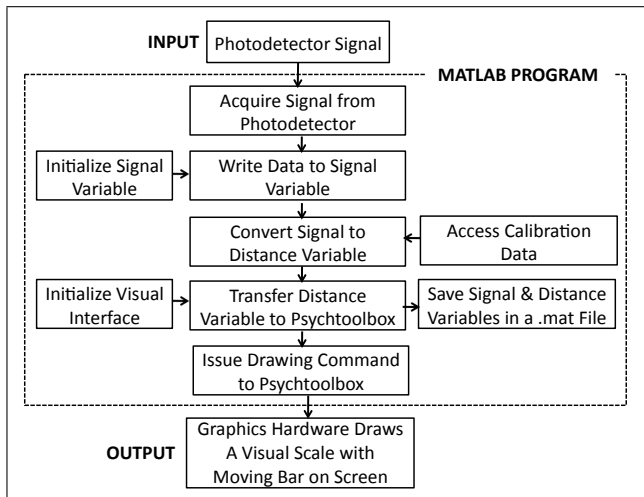


Fig. 3. Operational Software Block Diagram

IV. PRINCIPLE OF OPERATION

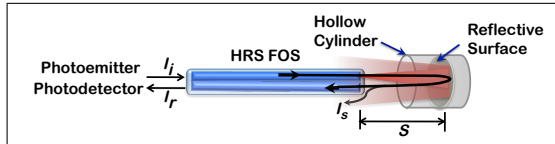


Fig. 4. Schematic diagram of the sensing principle. The reflective surface is placed at a distance S with respect to the probe's tip. It receives light from the tip of the fiber and reflects most of the light back into the fiber.

The principle of operation for this system is based on the measurement of the reflected light intensity as a function of position (distance) of the reflective surface placed in the optical path as shown in Fig. 4. A modulated LED produces a beam of light that propagates down the optical fiber and emits into the air at the outlet of the fiber tip. Incident light (I_i) reflects almost symmetrically with respect to the normal line with minimum light scattering (ΣI_s). The resultant reflected light ($I_r = I_i - \Sigma I_s$) is received by a photodetector. In the

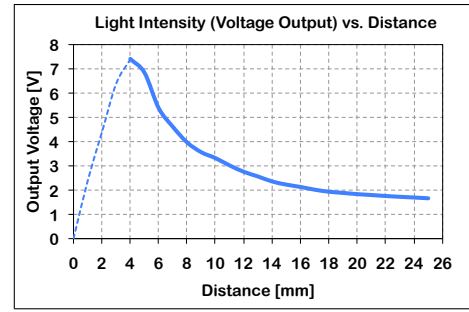


Fig. 5. Response of FUE 500C1003 FOS

initial state, the intensity of the reflected light is constant; however, actuation of any of the maneuvering elements by a participant (e.g., rotation of a wheel, pressing of a button) results in the displacement of the reflective surface leading to a change in the output analogue voltage of the photodevice. Fig. 5. shows the HRS sensor output function which can be divided into three regions: the front slope (dashed line), the transition (peak), and the back slope (solid line). Although front slope is more linear and sensitive, back slope is used for displacement measurement in HRS for the following reasons: 1) the back slope has a larger effective range, and 2) the gap between sensor tip and reflective surface in our configuration is always greater than 4 mm which makes it impossible to use the front slope region of the sensor output curve.

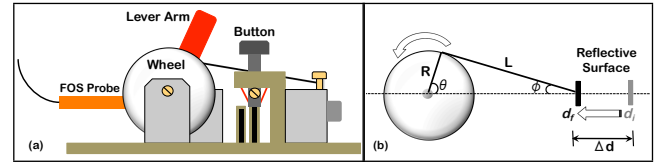


Fig. 6. (a) Arrangement of maneuvering elements in the optomechanical unit; (b) modified slider-crank mechanism for analog input module

In a binary input module, the maneuvering elements are hinged directly to the reflective plates. When a button is pressed its corresponding plate moves inside the optical path. Difference in the placement of the reflective plates in the optical path determines which button is pressed. In an analog input module, a modified slider-crank mechanism (Fig. 6. b), converts rotary motion of the wheel or lever arm to a linear movement of the reflective surface. The displacement of the reflective surface (i.e., $\Delta d = d_f - d_i$) can be determined from the geometry. Assuming $\theta = \phi = 0$ at the initial distance d_i :

$$\Delta d = R[1 - \cos(\theta)] + L[1 - \cos(\phi)] \quad (1)$$

Since $L^2 = [L\cos(\phi)]^2 + [L\sin(\phi)]^2$, and $L\sin(\phi) = R\sin(\theta)$, (1) can be simplified to:

$$\Delta d = R[1 - \cos(\theta)] + L - \sqrt{L^2 - [R\sin(\theta)]^2} \quad (2)$$

which leaves θ as the only angular variable required for calculation. If we define parameter $\lambda = R/L$, (2) is further rearranged to:

$$\Delta d = R \left[1 - \cos(\theta) + (1/\lambda) \left[1 - \sqrt{1 - (\lambda \sin(\theta))^2} \right] \right] \quad (3)$$

V. MRI COMPATIBILITY TEST

To investigate whether HRS interferes with the MRI signal during scanning, we carried out a series of test on a 3T Philips Ingenia scanner (Philips Healthcare, The Netherlands). Each set of experiments consisted of a cylindrical homogeneous water phantom filled with 1.7 gram/liter of nickel chloride and 7 gram/liter of sodium chloride imaged alone (baseline, condition (a)), and subsequently imaged under the following conditions: (b) with an input device turned off; (c) with a turned-on device without actuation of any of its maneuvering element; turned-on device with the actuation of its maneuvering elements including (d) rotation of a wheel; (e) movement of a joystick in one direction; and (f) pressing of a button continuously with a glass rod. Thirty four axial slices were acquired with echo-planar (EPI) (TR/TE = 2000/30, FOV = 24 cm, flip angle = 80°, acquisition matrix = 96 × 96, voxel size = 3 × 3 × 3 mm). For image quality, time-variant signal-to-noise ratio (tSNR) which is the ratio between the temporal mean and the temporal standard deviation of a time-series [12], was measured (Fig. 7). MR image quality was also evaluated with image subtraction method (Fig. 8). Overall tSNR decreased by no more than 2% across all conditions. No magnetically induced force or torque was observed when the input device was placed inside the scanner bore (about 50 cm away from the phantoms base) before and during the fMRI test.

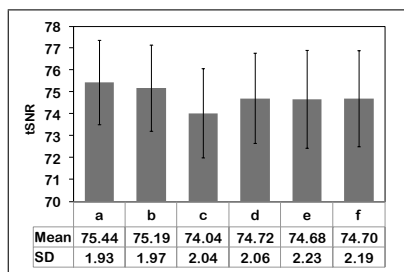


Fig. 7. tSNR measurements for six test conditions

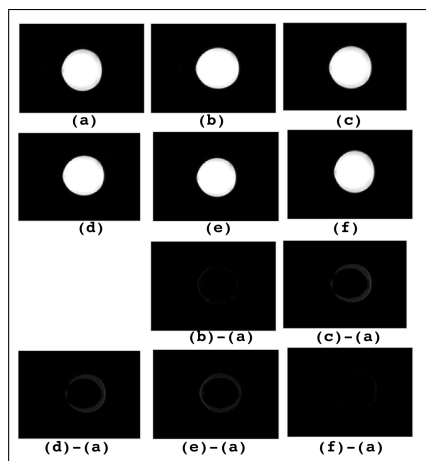


Fig. 8. (Top) A graphical representation of the imaging results; (Bottom) Image subtraction results with condition (a) as a baseline.

VI. PERFORMANCE AND ERGONOMIC EVALUATION

We measured the force and/or torque required to actuate maneuvering elements using a piezo-electric force transducer

(Kistler 9205, Switzerland) (Table 4). At a maximum 7 N force, this design fulfilled our MVC requirement. For optical signal reliability, we evaluated the sensor's output voltage with a digital multimeter (HP34401A, Hewlett-Packard) while actuating the analog module (Fig. 9). The variation of signal was less than 0.5 V.

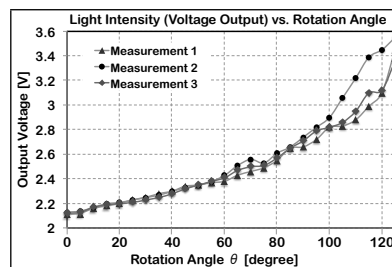


Fig. 9. HRS optical signal reliability

Configuration	Torque / Force
Wheel	6.35 ± 0.19 N.m (Radius = 2.5 cm)
Lever arm	2.41 ± 0.05 N.m (Handle = 12 cm)
Push button	3.69 ± 0.12 N (Surface area = 3.1 cm ²)

VII. CONCLUSION

A novel fiber-optic-based response system with visual interface was developed for use during an fMRI experiment. Aside from a desktop computer and a Matlab-based open-source software Psychophysics Toolbox for visual interface, the system costs about US\$718 to construct (Table 5).

TABLE 5. COST BREAKDOWN OF THE HRS HARDWARE

Component	Cost
FOS With 10m Optical Fiber	\$267
Photodiode With Build-in Amplifier	\$166
USB Data Acquisition Card	\$240
Misc. Electronics & Plastic Components	\$45
Total	\$718

REFERENCES

- [1] E. Amaro, G. Barker, *et al.*, "Study design in fmri: Basic principles," *Brain and cognition*, vol. 60, no. 3, pp. 220–232, 2006.
- [2] M. Tada and T. Kanade, "Development of an mr-compatible optical force sensor," in *Engineering in Medicine and Biology Society, 2004. IEMBS'04. 26th Annual International Conference of the IEEE*, vol. 1. IEEE, 2004, pp. 2022–2025.
- [3] J. Meinhardt and J. Müller, "Motor response detection using fiber optics during functional magnetic resonance imaging," *Behavior Research Methods*, vol. 33, no. 4, pp. 556–558, 2001.
- [4] G. Schaeffers, "Testing mr safety and compatibility: an overview of the methods and current standards." *IEEE engineering in medicine and biology magazine: the quarterly magazine of the Engineering in Medicine & Biology Society*, vol. 27, no. 3, p. 23, 2008.
- [5] D. Chaffin, G. Anderson, *Occupational Biomechanics*. Wiley, NY, 1984.
- [6] S. Chengalur, S. Rodgers, and T. Bernard, *Kodak's ergonomic design for people at work*. John Wiley & Sons, New York, 2004.
- [7] E. Tichauer and H. Gage, "Ergonomic principles basic to hand tool design," *The American Industrial Hygiene Association Journal*, vol. 38, no. 11, pp. 622–634, 1977.
- [8] S. Trewhin and H. Pain, "Keyboard and mouse errors due to motor disabilities," 1999.
- [9] M. Smith, J. Sharit, and S. Czaja, "Aging, motor control, and the performance of computer mouse tasks," *Human Factors: The Journal of the Human Factors and Ergonomics Society*, vol. 41, no. 3, pp. 389–396, 1999.
- [10] B. Kantowitz and G. Elvers, "Fitts' law with an isometric controller: Effects of order of control and control-display gain." *Journal of Motor Behavior*, 1988.
- [11] P. Van Wely, "Design and disease," *Applied Ergonomics*, vol. 1, no. 5, pp. 262–269, 1970.
- [12] R. Weisskoff, "Simple measurement of scanner stability for functional nmr imaging of activation in the brain," *Magnetic resonance in medicine*, vol. 36, no. 4, pp. 643–645, 2005.